To cite this version :

RESEARCH ARTICLE

SPE INSPIRING PLASTICS PROFESSIONALS   Polymer COMPOSITES   **WILEY**

Anomalous hydraulic fluid absorption by carbon fiber/PEKK composites: Physical and mechanical aspects

Gwladys Lesimple[1] | **Ilias Iliopoulos[1]** | **Guillaume Miquelard-Garnier[1]** [iD] |
Thibaut Benethuiliere[2] | **Stéphane Bizet[3]** | **Bruno Fayolle[1]** [iD]

[1]Laboratoire PIMM, Arts et Metiers Institute of Technology, CNRS, Cnam, HESAM Universite, Paris, France

[2]Hexcel Reinforcements, Les Avenières, France

[3]Arkema, Serquigny, France

Correspondence
Bruno Fayolle, Laboratoire PIMM, Arts et Metiers Institute of Technology, CNRS, Cnam, HESAM Universite, 151 boulevard de l'Hopital, Paris 75013, France.
Email: bruno.fayolle@ensam.eu

Funding information
BPI France, Grant/Award Number: PSPC.AAP-7.0_HAICoPAS

Abstract

Carbon fiber (CF)/polyetherketoneketone (PEKK) composites are exposed to Skydrol, a hydraulic fluid made of phosphate esters widely used in the aviation field. The present study investigates Skydrol absorption of CF/PEKK composite layups and the associated PEKK matrix. A significant unexpected increase of Skydrol uptake is observed for cross-ply composites (0.50%) compared to unidirectional ones (0.06%), independently of ply number. The use of 'model' fluids like water and ethanol allows to identify the origin of this anomalous Skydrol absorption in the case of cross-ply layup. We propose that the latter involves an imbibition process governed by the fluid surface tension and the presence of submicronic cavities. SEM imaging of composite cross-section after ion beam polishing confirms fiber-matrix submicronic debonding in the interlaminar region in the cross-ply composite. SEM–EDX confirms the presence of Skydrol into the submicronic cavities. Despite this anomalous absorption, off-axis tensile testing as well as ILSS testing show no significant impact of Skydrol on CF/PEKK mechanical properties with less than 10% difference compared to the initial values.

Highlights

- Absorption by diffusion of Skydrol in neat PEKK and CF/PEKK composites
- Link between fluid surface tension and anomalous Skydrol absorption
- Evidence of submicronic cavities in CF/PEKK composites by means of SEM–EDX
- Low impact of Skydrol on CF/PEKK mechanical properties

KEYWORDS

absorption, CF/PEKK, composite, hydraulic fluid, mechanical properties, microstructure, Skydrol

1 | INTRODUCTION

Polyaryletherketones (PAEK) are being of most interest to replace thermoset matrices in carbon fiber reinforced composites especially for aeronautics.[1,2] These high performances thermoplastics provide excellent thermal, chemical and mechanical properties while requiring easier storage conditions than thermosets like epoxies and

are inherently flame retardant.[3,4] Their glass transition temperature (T_g) is over 140°C while their melting temperature (T_m) exceeds 300°C.[4] Due to their thermoplastic nature, composites based on PAEK are potentially recyclable, weldable and can be consolidated out of autoclave or in-situ.[4–10]

Polyetheretherketone (PEEK) is the most studied PAEK matrix with numerous references on crystallization, aging, mechanical properties, etc.[9,11–17] In the last decades, polyetherketoneketone (PEKK) has been developed to compete with PEEK as a matrix for structural composite parts of aircrafts. This copolymer offers the possibility to modulate its melting temperature while keeping a constant glass transition temperature.[18] This characteristic arises from its chemical composition as it consists of two types of isomers: TT (terephtaloyle-terephtaloyle dyad) and TI (terephtaloyle-isophtaloyle dyad). A higher T/I ratio leads to a higher melting temperature. Thereby, PEKK with a 70/30 T/I ratio has a melting temperature of 332°C, far enough from its degradation temperature (estimated around 410°C[18]) to be processed easily and is used as matrix for high performances thermoplastic composites.[4,9,19]

Composite parts can be exposed to different fluids during maintenance as well as in the case of a leak. When a new composite matrix is considered, like PEKK here, it is of importance to determine its chemical resistance, especially to aeronautic fluids. Hydraulic fluids such as Skydrol, a mixture of three different phosphate esters (tributyl, dibutyl phenyl and diphenyl butyl phosphates) with some other additives in a smaller proportion,[20,21] are known to be aggressive for thermosets like epoxies.[22–25] For instance, Buggy et al.[25] record a weight gain of 1.46% of an epoxy resin immersed in Skydrol at room temperature. La Saponara[26] shows that the weight gain is highly dependent of temperature (0.3% at room temperature versus 2% at 70°C). Other studies focus on the effect of Skydrol on epoxy adhesive bonding of composites. Sugita et al.[22] observe a coloration as well as swelling of the adhesive with immersion in Skydrol. Moreover, the mechanical and adhesive properties are negatively affected.[22–24]

In comparison, very few studies report the effect of Skydrol on neat PAEK or CF/PAEK composites. Stober and Seferis[27] measure a weight gain at saturation of 1.1% of a crystallized unreinforced PEEK film immersed in Skydrol. Concerning PEKK, Dominguez[28] shows that the elastic modulus and ultimate tensile strength of unreinforced PEKK exposed to Skydrol remain unchanged. Little literature focusses on the effect of hydraulic fluids on CF/PAEK composites. Horn et al.[29] report a hydraulic fluid (type not specified) uptake of 0.25% of a quasi-isotropic CF/PEEK composite but no saturation plateau is reached. Ma et al.[30] also studied the uptake of both unidirectional and woven CF/PEEK immersed in a

petroleum-based hydraulic fluid and measure an uptake lower than 0.5%. Only one study was found, addressing the weight gain of CF/PEEK immersed in Skydrol. Pritchard and Randles[31] report a 0.7% weight gain at saturation of CF/PEEK exposed to Skydrol.

In this study, the quantity of Skydrol absorbed is then determined in both neat PEKK and CF/PEKK. The Skydrol absorption is studied for both unidirectional and cross-ply CF/PEKK composites and is compared to a 'model' fluid (ethanol). SEM imaging is perfomed to get a better understanding of the difference in microstructure between the two types of layup. Finally, possible impact of fluids absorption on the composites mechanical properties is investigated by probing the fiber-matrix interface through off-axis tensile testing and the ply-ply interface through short beam shear testing. The impact of Skydrol on the bulk matrix properties is evaluated by tensile test experiments.

2 | EXPERIMENTAL

2.1 | Materials

Neat PEKK Kepstan 7002 (T/I ratio of 70/30) is provided by Arkema in the form of injected plates ($100 \times 100 \times 2$ mm³) and mechanical specimens (2 mm-thick ISO 527 specimens). CF/PEKK unidirectional tapes are provided by Hexcel Reinforcements. The tapes contain 66 wt% carbon fibers and have a thickness of 200 μm. Unidirectional composites of 4, 8 and 24 plies ($[0]_4$, $[0]_8$, $[0]_{24}$) as well as cross-ply laminates of 8 and 24 plies ($[0/90]_{2s}$ and $[0/90]_{6s}$) are manufactured using the 'vacuum-bag-only' (VBO) method. The consolidation cycle of the layups is performed in an oven at 390°C during 90 min. Cooling is carried out using pressurized air with a pressure regulator to control the cooling rate. DSC measurements on the final composite parts (see Figure S1) show a single crystallization peak, no cold crystallization and a melting enthalpy of $\Delta H_{m,CF/PEKK} = 12{,}8 \pm 1$ J.g⁻¹ corresponding to the enthalpy of a fully recrystallized neat PEKK sample ($\Delta H_{m,PEKK} = 38{,}5 \pm 1$ J.g⁻¹, Figure S2). Consequently, all composites manufactured are considered to have reached a maximum crystallinity.

The gravimetric measurements are performed by immersing composite samples in three different fluids: deionized water (VWR), ethanol (VWR) with a purity of 96% and Skydrol LD-4 (Eastman, kindly provided by Hexcel). Table 1 gives the main characteristics of water, ethanol and tributyl phosphate (TBP) which represents the main constituent of Skydrol.

	Water	Tributyl phosphate	Ethanol
Molar mass (g.mol^{-1})	18	266	46
Molar volume at 20°C (cm^3.mol^{-1})	18	272	58
Surface tension at 20°C (mN.m^{-1})	72	28	22

TABLE 1 Molar mass, molar volume and surface tension of the three fluids.

TABLE 2 Number of samples used for gravimetric measurements in Skydrol and ethanol.

	PEKK	$[0]_8$	$[0]_{24}$	$[0/90]_{2s}$	$[0/90]_{6s}$
Skydrol	5	2	2	2	2
Ethanol	3	-	-	4	-

2.2 | Gravimetric measurement

Gravimetric measurements are performed both on neat PEKK and on CF/PEKK composites (8 and 24 plies). Square samples (50 × 50 mm^2) are cut from the neat PEKK and CF/PEKK plates using a diamond wire saw. The edges are smoothen using sand paper. The fact that edge effects are non-negligible in composite materials fluid absorption is crucial here. This is the reason why we first tried to seal the samples' edges. Nevertheless, no sealing solution was able to resist to Skydrol during long-term exposures. Skydrol is a relatively aggressive fluid to which most materials do not resist (for example the adhesive of aluminum tape). To overcome this experimental bias, the samples were carefully cut with a wire diamond saw in order to avoid inducing damages on the edges. Secondly, we varied the thickness of the samples (UD and 0/90). 8-ply layups have a thickness of 1.6 mm and 24-ply layups have a thickness of ca. 4.8 mm, to compare samples satisfying the 1/20 ratio for diffusion process with samples where side effects will be favored.

The samples are first dried in an oven under vacuum at 120°C during 48 h then crystallized in a classic oven at 200°C during 4 h to ensure full crystallization. WAXS measurements on the neat PEKK samples, using the methodology described by Tencé-Girault et al.,[32] provide a weight crystallinity of 19% corresponding to the maximum crystallinity of PEKK.[32,33] Aging is performed by immersion in Skydrol at 70°C and in ethanol at 25°C. The samples are placed in glass jars (sealed by a rubber sealant) in a water bath in order to control the aging temperature. The rubber sealant must be changed regularly because Skydrol degrades the rubber. Table 2 reports the number of PEKK and CF/PEKK samples immersed in Skydrol and ethanol for the gravimetric measurements. Unfortunately, the quantity of material supplied was not enough to ensure five samples per condition. Preliminary studies on thinner samples as well as the PEKK immersions in

Skydrol show very good repeatability of the gravimetric measurement. We then considered two samples would be enough to determine the Skydrol uptake in thicker laminates. All data points are provided in the following graphs except for PEKK immersed in Skydrol where the values presented are averaged.

Gravimetric measurements are performed regularly by taking the samples from the fluid, swabbing the surface to remove all liquid and weighing them using a Mettler Toledo analytical balance. The mass percentage of fluid absorbed (w) at time t is calculated using Equation (1):

$$w = \frac{m - m_0}{m_0} \times 100 \qquad (1)$$

where m is the mass of the sample at time t and m_0 the initial mass of the sample in the dry state.

2.3 | Mechanical tests

2.3.1 | Tensile test

Neat PEKK ISO 527 1BA 2-mm thick specimens are tested on an Instron 5966 machine at a speed of 1 mm/min using a cell force of 10 kN. The specimens are tested in the dry state (dried and crystallized as described in section 2.2) and after immersion in Skydrol at 70°C (as per section 2.2) from 500 to 3000 h. Aged specimens are dried with a paper towel prior to mechanical testing. The nominal displacement is recorded as the crosshead displacement.

2.3.2 | Off-axis tensile test

The fiber-matrix interface is mechanically stressed using the off-axis tensile test. Specimens are cut in $[0]_4$ CF/PEKK plates using a water jet at an angle of 10° with respect to the fibers direction. Their dimensions are 278 mm × 12.7 mm according to Chamis and Sinclair.[34] Ten of the specimens are immersed in Skydrol in a large glass dish placed in an oven at 70°C during 1000 h.[35]

The specimens are tested at 23°C using an Instron 5581 apparatus at a speed of 2 mm/min using a 50 kN cell force. Results are averaged over six specimens for the

dry state and ten for the aged ones. In order to measure the deformation in the carbon fiber direction (10°), the tensile test is coupled with 2D digital image correlation (DIC). The specimens are covered with a random black and white speckle pattern using spray paint. The specimen deformation is captured using a Manta G-917B camera with a telecentric lens and a LED panel. An acquisition box (KiloNewton) is used to save data from the camera (captured images) and the tensile testing machine (applied force and nominal displacement). A picture is captured every 100 ms. The DIC data are recorded and analyzed using respectively VIC-snap and VIC2D softwares (KiloNewton). The step size and subset size are chosen to be 12 and 27 pixels respectively, as recommended by.[36] The shear stress (τ_{12}) is computed as[37]:

$$\tau_{12} = \sigma_x \cos\theta \, \sin\theta \quad (2)$$

With σ_x the stress in the loading direction and θ the angle of the fibers (here $\theta = 10°$).

The shear strain (ε_{12}) is calculated such that[34]:

$$\varepsilon_{12} = (\varepsilon_{yy} - \varepsilon_{xx})\sin 2\theta + \varepsilon_{xy}\cos 2\theta \quad (3)$$

With ε_{xx}, ε_{yy} and ε_{xy} the shear strains in the tensile testing machine landmark. The shear modulus (G_{12}) is calculated in the range $\varepsilon_{12} \in [0.2\%–0.6\%]$ as per.[37]

2.3.3 | ILSS

The interlaminar shear strength (ILSS) of the composite is measured using the short beam shear test (ASTM D2344). The specimens are cut from the 24-ply laminates using a diamond wire saw. Depending on the thickness of the laminate, the specimen length is equal to six times the thickness and the width is equal to twice the thickness. The test is performed on an Instron 5581 apparatus, at 1 mm/min using a 50 kN cell force. The setup including the three cylinders only support a maximum load of 10 kN. The results are averaged on six specimens. The ILSS is measured as:

$$ILSS = \frac{3F_{max}}{4hw} \quad (4)$$

With F_{max} the maximum load applied, h the specimen thickness and w the specimen width.

The samples are tested at 23°C, in the dry state and after 3500 h of immersion in Skydrol at 70°C.

2.4 | SEM

Scanning electron microscopy (SEM) is performed on a Thermo Fisher Quanta FEG 250 microscope at Arkema. The cross-section surfaces of 8-ply UD and cross-ply samples are prepared by ion beam polishing using a Gatan Ilion+693 apparatus under vacuum at 6 keV. The cross-ply samples surfaces are prepared using ionic polishing in order to avoid degrading the sample surface. Previous tests have indeed shown carbon fibers breaking when using mechanical surface preparation. As PEKK is more ductile than carbon fibers, sand papers and diamond solutions create cavities in the matrix phase. The polished surface is in the thickness direction in order to exhibit different plies and has a surface of around 400×400 μm^2.

Energy-dispersive x-ray spectroscopy (SEM–EDX) is also performed with the same apparatus. The ion beam polished sample is aged in Skydrol by immersion at 70°C during ca. 15 h. The sample is gently surface dried prior to observation. The microscope is set under low vacuum (80 Pa) in order to avoid desorption of the Skydrol remaining in the composite, with a beam energy of 10 keV. Phosphorus mapping of the sample surface is carried out in order to determine where the Skydrol is present in the composite microstructure as this fluid is composed of phosphate esters. The mapping is performed during ca. 10 min to avoid degradation of the composite that occurs at longer durations.

3 | RESULTS AND DISCUSSION

3.1 | Skydrol absorption

3.1.1 | Neat PEKK

The weight gain of neat crystallized PEKK immersed in Skydrol at 70°C is shown in Figure 1. The values are compared to water, a fluid that was the focus of a previous study.[33] The weight gain is plotted against the square root of time in order to observe the potential linear relationship at short times (typical of a fickian absorption behavior). The timescale is divided by the sample thickness to allow for easier comparison between different experiments.

The standard deviation of the experimental data is of the order of 0.02% for both water and Skydrol exposures. Skydrol diffusion in neat PEKK is particularly slow and does not reach saturation within the current exposure time. Neat PEKK absorbs about 0.9% of water at saturation,[33] which corresponds to 800 h of exposure of a 2 mm-thick plate whereas it absorbs only 0.27% of Skydrol after 7200 h. As stated before, to the best of our knowledge, there is no data for PEKK immersed in Skydrol. Stober and Seferis[27]
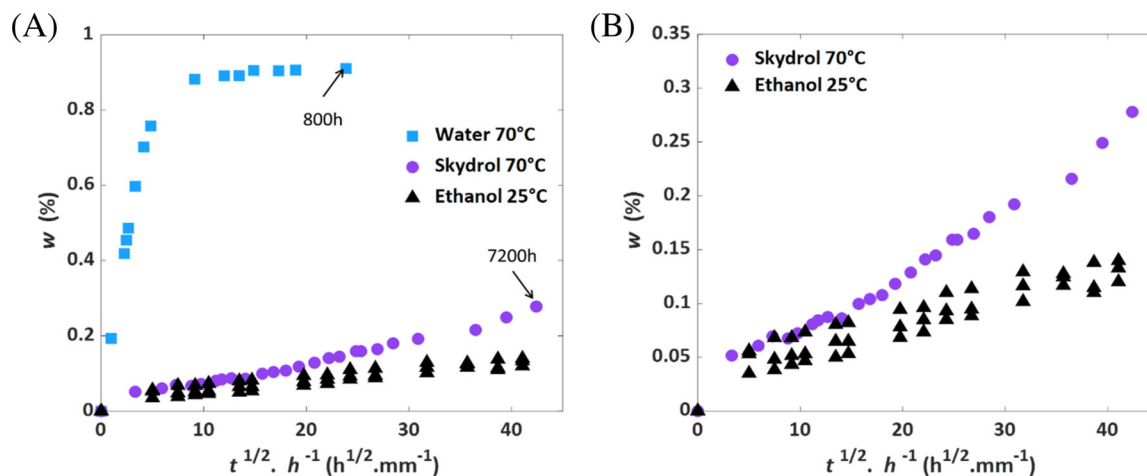
FIGURE 1 (A) Weight gain as a function of the square root of time divided by the sample thickness of neat PEKK immersed in water (70°C), Skydrol (70°C) and ethanol (25°C). (B) Zoom in the plot showing data for Skydrol (70°C) and ethanol (25°C) only.

find a saturation value for a 60 µm-thick film of crystallized PEEK immersed in Skydrol at 70°C of 1.1%. Nevertheless, this value does not seem to be consistent with the absorption curve determined for PEKK in the present study. Indeed, the saturation value of 1.1% would not be reached with the current diffusion rate observed in this study.

The absorption rate is discussed hereafter instead of considering the diffusion coefficient, as there is no saturation plateau in the case of Skydrol. The rate of sorption of water by PEKK (0.18 mm.h$^{-1/2}$) is 30 times higher than that of Skydrol (0.006 mm.h$^{-1/2}$), which may be linked to the size of the penetrant molecules. Tributyl phosphate being the main component of Skydrol, the chemical characteristics of the fluid will be considered those of TBP. Table 1 gives the molar mass of water and Skydrol, showing a significant difference between the two fluids.

3.1.2 | Unidirectional and cross-ply CF/PEKK

Unidirectional and cross-ply 8 and 24-ply composites (respectively 1.6 and ca. 4.8 mm thick samples) are immersed in Skydrol at 70°C in order to determine the effect of ply orientation as well as layup thickness on Skydrol transport in the CF/PEKK composites. Figure 2 shows the weight gain as a function of the square root of time divided by the sample thickness of these composites in Skydrol for 8 and 24-ply unidirectional composites ([0]$_8$ and [0]$_{24}$) and 8 and 24-ply cross-ply composites ([0/90]$_{2s}$ and [0/90]$_{6s}$).

No saturation plateau is reached for any of the samples. Moreover, the diffusion does not follow a fickian nor a pseudo-fickian behavior for the cross-ply

composites for Skydrol exposure as the weight gain as a function of the square root of time is not linear at short times (Figure 2A). For these composites, the Skydrol absorption between 8 and 24-ply composites shows a significant discrepancy in terms of weight gain after ca. 13 h$^{1/2}$.mm^{-1} with an uptake of 0.34% and 0.40% for 8 and 24 plies respectively. This discrepancy can be associated to edge effect during the absorption process. More precisely, this is probably due to interlaminar cavities accessible to the fluid through the edges of thick samples. This phenomenon has already been discussed in the previous study in the case of water.[38] This difference in Skydrol uptake between 8 and 24-ply samples is observed for both UD and cross-ply layups.

The unidirectional composites absorb around 0.06% of Skydrol (Figure 2B) while the cross-ply CF/PEKK samples absorb up to ten times more Skydrol after 4000 h (w$_{4000h}$ = 0.50% for the [0/90]$_{2s}$ composite). The Skydrol uptake measured for the cross-ply composites is consistent with the value reported by Pritchard and Randles for quasi-isotropic CF/PEEK (0.7%).[31] It was evidenced by microscopy image analysis that the composites used contain less than 0.1 v% porosities with characteristic dimensions superior to >1 µm (Figure S3). Thus, the excess of Skydrol absorbed by the cross-ply composites cannot be explained by these porosities. It should also be stated that this difference in quantity of Skydrol absorbed by UD and cross-ply composites has already been observed in the case of water but in a smaller proportion (about 0.1% difference).[38] Skydrol seems to have more ability to penetrate the cross-ply composites compared to unidirectional ones. This observation leads to the hypothesis that smaller porosities (<1 µm) are present in the cross-ply CF/PEKK composites.
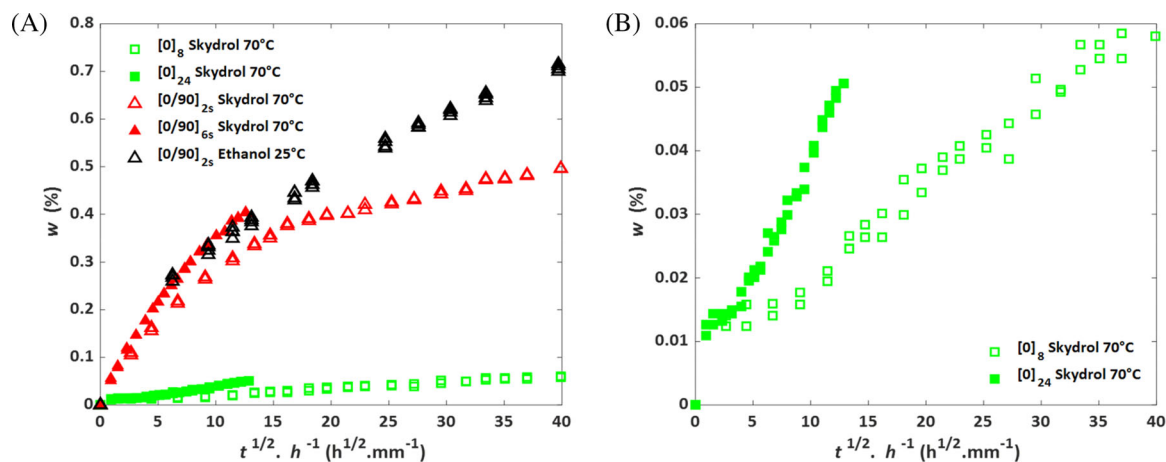
FIGURE 2 Weight gain as a function of the square root of time divided by the sample thickness of (A) CF/PEKK composites immersed in Skydrol (70°C) and ethanol (25°C, black symbols), (B) unidirectional composites only (zoom from Figure 2A), immersed in Skydrol at 70°C.

An imbibition process involving very small porosities could then occur in the cross-ply composites.

Let us recall that imbibition is a physical phenomenon describing the penetration of a liquid in a capillary at a given pressure. The smallest capillary radius (R) that will be penetrated is equal to the surface tension of the fluid (γ) over the applied pressure (P), as given in Equation (4):

$$R = \frac{2\gamma}{P} \qquad (5)$$

In the field of composites and their interaction with fluids, authors have proposed to take into account the capillarity process induced by the presence of porosity and cracks to simulate the absorption process. In this context, we can cite the work of Weitsman and Guo[39] or more recently Gagani et al.[40] It should be noted here that our approach to analytically model the imbibition process is limited to a capillary-type geometry (equation 4). We could, for example, modify this modeling by taking into account the shape or aspect ratio of porosities measurable by synchrotron x-ray microtomography. In particular, the aim could be to identify the porosity network and its shape factor as a function of ply orientation and out-of-autoclave consolidation conditions.

In the present study, the surface tension of TBP, the main component of Skydrol, is close to three times lower than that of water (Table 2). Thus, if we consider an imbibition process under atmospheric pressure, the minimal radius of a capillary that can be penetrated by water is on the order of 1.4 μm whereas it is of 0.5 μm in the case of Skydrol. In other words, composites will absorb more Skydrol if submicronic porosities, such as those that could

occur during fiber-matrix debonding, are present. To validate if this Skydrol absorption is governed by the presence of very small porosities, we propose to replicate the experiments by replacing the Skydrol by ethanol.

3.2 | Ethanol as a 'model' fluid

In order to confirm the effect of the fluid's surface tension on the absorption behavior, ethanol is used as a 'model' fluid, with a surface tension close to the one of TBP but a molecular weight close to the one of water. Neat PEKK is immersed in ethanol at 25°C (not at 70°C as for Skydrol because of the boiling temperature of ethanol) and the weight gain is presented in Figure 1. Even if the molar mass of ethanol is closer to the one of water, neat PEKK does not absorb much more fluid. Under the current exposure temperature, ethanol absorption rate by PEKK is of the same order of magnitude as Skydrol.

Samples of [0/90]$_{2s}$ composite are immersed in ethanol (at 25°C) in order to compare the absorption behavior with the one of Skydrol (Figure 2). Even with a lower exposure temperature, the uptake of ethanol by the cross-ply composite follows roughly the same behavior as Skydrol with a greater amount of fluid uptake. The aforementioned study by Pritchard and Randles[31] compares the weight uptake of Skydrol and isopropanol of a quasi-isotropic CF/PEEK 8-ply composite at 23°C. The authors show that the diffusion rates are equivalent at short times for the two fluids but diverge at a certain point. Likewise, the weight gain measured at saturation is also equivalent. Unfortunately, it is not possible to confirm the last observation as saturation is not reached in the present study. Nevertheless, the ethanol uptake
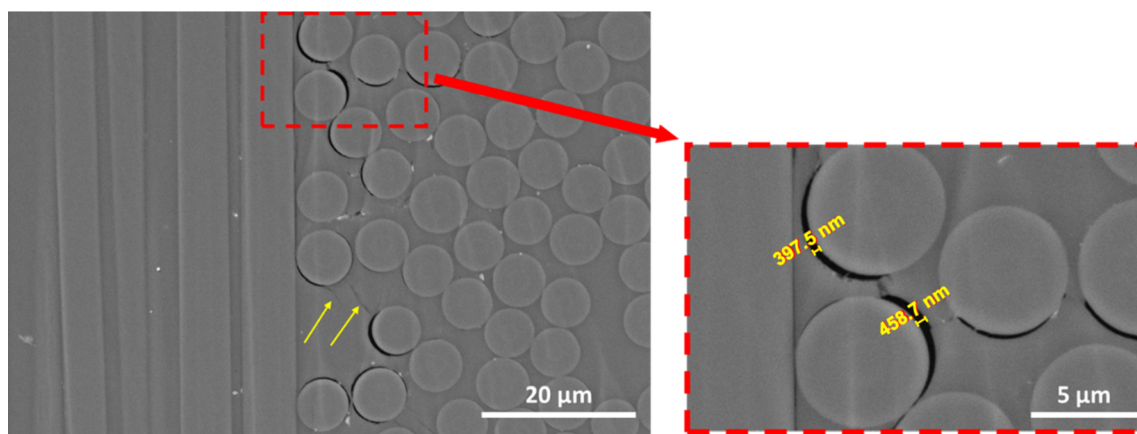
FIGURE 3   SEM image of the interply region of a $[0/90]_{2s}$ CF/PEKK composite.

confirms that the fluid surface tension appears to be the main parameter governing the abnormal uptake by the cross-ply composite compared to the unidirectional one.

3.3 | Composite microstructure

The water, Skydrol and ethanol uptakes obtained for the cross-ply composites (cf Figure 2) lead to the hypothesis that a submicronic porosity is present in these composites, but absent in the unidirectional ones. The difference of fluid uptake between UD and cross-ply composites would be indeed less important in the case of water as the high surface tension of water does not allow fluid penetration in the submicronic cavities. To confirm this hypothesis, SEM imaging is used to observe the interply region in particular, as it constitutes the main difference between cross-ply and UD composites structure.[23]

SEM images in Figure 3 show several cavities under the shape of fiber-matrix debonding only in the interlaminar regions, having a width of ca. 500 nm, in good quantitative agreement with the theoretical prediction from the simple imbibition model. Cracks are also observed in the matrix phase in these regions.

These debondings and cracks are the consequence of residual stresses (due to matrix shrinkage) remaining in the cross-ply composite that are dependent on the cooling rate.[41] Tsukada et al.[42] reported the macroscopic parabolic aspect of the residual stresses in unidirectional thermoplastic composite. Cooling of the plate surface is faster than in the bulk. Thus, compression stresses appear at the surface while tensile stresses develop in the bulk. At a smaller scale, the difference in fiber orientation between two consecutive plies and PEKK thermal shrinkage taking place in different directions lead to important stresses. These stresses are particularly concentrated in

the interply region. Indeed, the coefficient of thermal expansion of carbon fibers ($\alpha_T \approx 7$ to 12.10^{-6} K^{-1} for high strength carbon fibers) is negligible compared to that of PEKK ($\alpha_T \approx 230.10^{-6}$ K^{-1} for T > T$_g$).[19,43–46] If the residual stresses are greater than the fiber-matrix adhesion strength, debonding takes place during composite cooling after consolidation. On the contrary, cracks in the matrix phase will occur if the fiber-matrix adhesion is strong enough.[45]

As Skydrol is composed of phosphate esters, phosphorus mapping is performed by SEM–EDX in order to conclude if Skydrol can penetrate these cavities. Figure 4A shows the SEM image of a $[0/90]_{2s}$ composite after immersion in Skydrol for 15 h and Figure 4B shows the associated phosphorus mapping. One can see that the bluest areas of the mapping image correspond to the debondings observed on the corresponding SEM image. This result confirms the ability of Skydrol to penetrate these small porosities. Similar SEM observation and phosphorus mapping on unidirectional composites show no debonding nor presence of phosphorus in the UD composite exposed to Skydrol.

As a consequence, Skydrol could be used to determine the porosity of a sample. Considering that the density of Skydrol is equal to 0.97 g.cm^{-3} at 70°C and that the PEKK matrix absorbs ca. 0.06 wt% Skydrol, a sample of CF/PEKK which absorbs 0.4 wt% of Skydrol has a void content (porosities of size <1 μm) close to 0.3 v%.

Finally, a longer immersion time of cross-ply composites in Skydrol seems to relax the residual stresses. Indeed, when comparing SEM images of a $[0/90]_{2s}$ CF/PEKK composite before and after exposure to Skydrol, the width of the debondings have increased (Figure 5). This widening of the cavities during exposure could explain the absence of saturation plateau observed for Skydrol and ethanol uptakes of CF/PEKK composites (Figure 2).
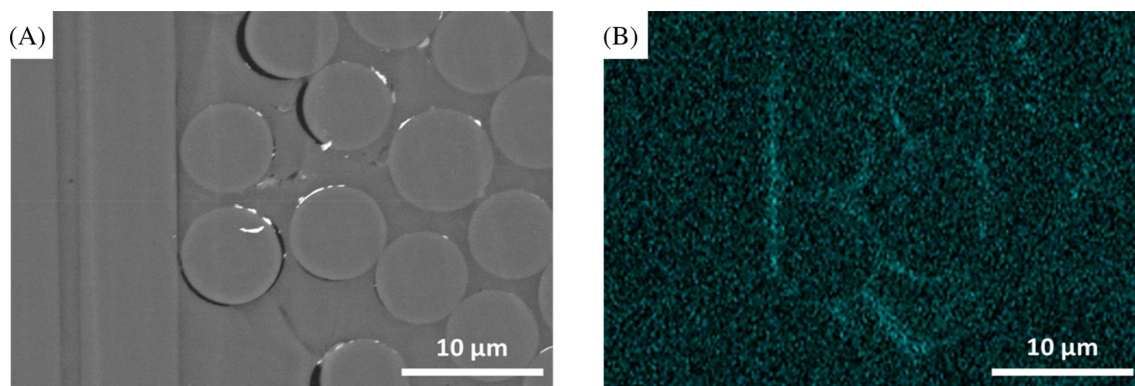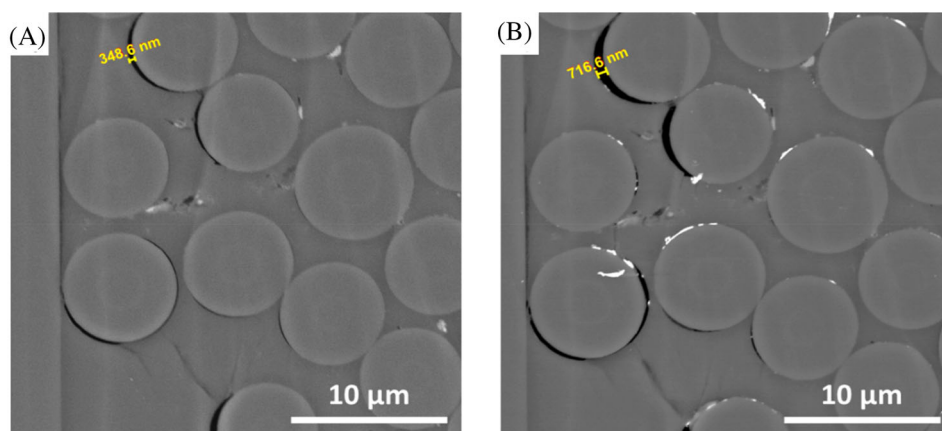
FIGURE 4 SEM (A) image and (B) phosphorus mapping of a [0/90]$_{2s}$ CF/PEKK composite after immersion in Skydrol at 70°C.

FIGURE 5 SEM images of a [0/90]$_{2s}$ composite (A) before aging and (B) after 15 h of immersion in Skydrol at 70°C.

3.4 | Mechanical properties of CF/PEKK exposed to Skydrol

The unexpected Skydrol absorption in the case of cross-ply composites is attributed to an imbibition process in submicronic cavities in the interply region due to fiber-matrix debonding caused by residual stresses after consolidation. It is then crucial to check possible consequences of this Skydrol absorption on the composites mechanical properties. For this purpose, we propose first to investigate tensile properties of neat PEKK to verify if matrix is affected by the Skydrol, and then the fiber-matrix interface before and after Skydrol exposure. To characterize fiber-matrix interface, off-axis tensile testing is proposed whereas short beam shear is performed to characterize the interply.

3.4.1 | Neat PEKK

Tensile testing of neat PEKK exposed to Skydrol at 70°C up to 3000 h shows no significant effect of the fluid on mechanical properties of the polymer (Figure 6). This can be understood due to the very low quantity of Skydrol absorbed by PEKK (cf Figure 1).

2 mm-thick PEKK samples absorb around 0.17% of Skydrol after 3000 h of exposure. The maximum effects seem to have already been reached after 500 h of immersion. The nominal elastic modulus decreases by 3% whereas the ultimate tensile strength decreases by 5%. The tensile tests have a good repeatability with a standard deviation ranging from 15 to 60 MPa on Young's modulus and of less than 1 MPa on ultimate tensile strength.

3.4.2 | Fiber-matrix interface

The effect of Skydrol on the fiber-matrix interface is studied by off-axis tensile testing on unidirectional composite exposed to Skydrol at 70°C during 1000 h. The shear modulus and shear strength are determined for an angle of 10° to the fibers direction and are reported in Table 3.

The shear modulus and shear strength measured for CF/PEKK are slightly higher than for CF/epoxy according to Merzkirch and Foecke results ($\tau_{12} = 65.6$ MPa for a CF/epoxy UD composite reinforced with 50 v% fibers).[47]
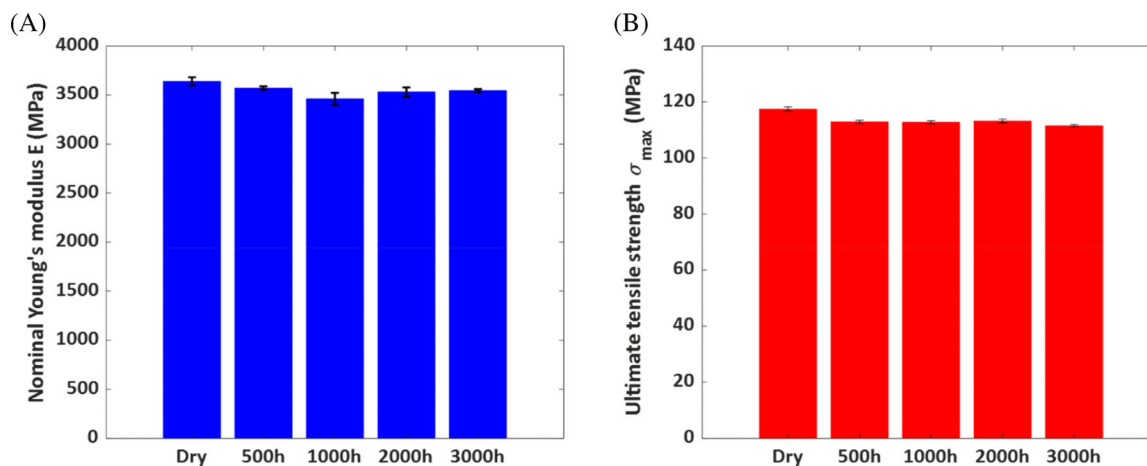
(A)

(B)

FIGURE 6 Young's modulus (A) and ultimate tensile strength (B) of PEKK in the dry state and for different immersion durations in Skydrol at 70°C.

TABLE 3 Shear modulus and shear strength of CF/PEKK in the dry state and after immersion in Skydrol at 70°C.

	DRY (0 h)	1000 h	w_{1000h} (%)
Shear modulus G_{12} (GPa)	7.5 ± 0.2	7.6 ± 0.2	$\sim 0.05\%$
Shear strength τ_{12} (MPa)	81 ± 3	81 ± 2	

TABLE 4 ILSS of unidirectional and cross-ply CF/PEKK in the dry state and after 3500 h immersion in Skydrol at 70°C.

	Layup	DRY (0 h)	3500 h	w_{3500h} (%)
ILSS (MPa)	$[0]_{24}$	96 ± 1	95 ± 2	$\sim 0.05\%$
	$[0/90]_{6s}$	88 ± 3	80 ± 2	$\sim 0.40\%$

The current results show that there is also no effect of the fluid on the fiber-matrix interface mechanical properties due to the low Skydrol uptake of UD CF/PEKK composite. The stress-train curves can be found in Figure S4.

3.4.3 | Interlaminar mechanical properties

ILSS is used to determine the impact of Skydrol on the interlaminar mechanical properties. Table 4 reports the ILSS of both UD and cross-ply composites in the dry state and after 3500 h of immersion in Skydrol at 70°C. ILSS is usually determined on UD composites but measuring the ILSS of cross-ply CF/PEKK gives a relative result of the impact of Skydrol on this type of layup. As expected, Skydrol has no impact on the ILSS of UD composites, as the latter absorbs only a minor amount of Skydrol ($w_{3500h} \approx 0.05\%$).

Nevertheless, a decrease of 10% of the ILSS of the cross-ply composite is observed indicating an effect of Skydrol on the interlaminar region. We can conclude that a Skydrol absorption associated to submicronic cavities does not lead to drastic properties changes. Although some Skydrol absorption can be detected for the cross-ply samples inducing some widening of the interfacial cavities (Figure 5), this effect has only a limited impact on the interlaminar mechanical properties. This result confirms the interest of such thermoplastic composites as a structural material for aerospace applications.

4 | CONCLUSIONS

This study focused on the possible interaction between Skydrol and CF/PEKK composites. As for neat PEKK, unidirectional CF/PEKK absorbs very little Skydrol (<0.1%). Nevertheless, immersion of cross-ply composites show a Skydrol uptake ten times higher. This difference is not explained by the amount of porosities determined by optical microscopy, which is <0.1% for both layups. The comparison of fluid uptake with a 'model' fluid like ethanol that have a smaller molar mass than tributyl phosphate (main component of Skydrol) but similar surface tension confirms that the latter is the key phenomenon to understand the abnormal uptake. SEM images of cross-ply composite samples evidence fiber-matrix debonding, particularly in the interlaminar region, confirming an imbibition-based scenario for this abnormal uptake. The submicronic cavities are caused by residual stresses that concentrate at the interface between to plies oriented with different angles. These residual stresses are partly released upon cooling after consolidation of the composite and create fiber-matrix debonding if the adhesion is non-optimal. Phosphorus mapping proves that Skydrol is able to penetrate these

debondings, confirming further the imbibition scenario. As a result, Skydrol absorption can be used as a tracer to detect submicronic cavities associated to the debonding process. Furthermore, we have shown that ethanol, a solvent easier to manipulate than Skydrol, can be also used to detect the submicronic damage. Complementary studies by x-ray microtomography are planned to explore in details and in-situ the shape and position of these residual cavities.

From a mechanical point of view, Skydrol absorption consequences on mechanical properties, specific tests characterizing matrix-fibers interfaces have been performed. The results show that Skydrol has no impact on neat PEKK nor CF/PEKK unidirectional mechanical properties as this type of layup does not absorb Skydrol. On the other hand, a moderate decrease of ILSS, about 10%, is observed for the cross-ply composites upon absorption of Skydrol. From all these observations, we can conclude that Skydrol absorption doesn't affect significantly the mechanical behavior of CF/PEKK composites.

CONFLICT OF INTEREST STATEMENT

The authors declare no conflict of interest.

DATA AVAILABILITY STATEMENT

Data are available on request.

ORCID

Guillaume Miquelard-Garnier https://orcid.org/0000-0002-0251-8941

Bruno Fayolle https://orcid.org/0000-0002-9578-1692

REFERENCES

1. Barile M, Lecce L, Iannone M, Pappadà S, Roberti P. Thermoplastic composites for aerospace applications. In: Pantelakis S, Tserpes K, eds. *Revolutionizing Aircraft Materials and Processes*. Springer International Publishing; 2020:87-114. doi:10.1007/978-3-030-35346-9_4

2. Veazey D, Hsu T, Gomez ED. Next generation high-performance carbon fiber thermoplastic composites based on polyaryletherketones. *J Appl Polym Sci*. 2017;134:134. doi:10.1002/app.44441

3. Vaidya UK, Chawla KK. Processing of fibre reinforced thermoplastic composites. *Int Mater Rev*. 2008;53:185-218. doi:10.1179/174328008X325223

4. Arquier R, Iliopoulos I, Régnier G, Miquelard-Garnier G. Consolidation of continuous carbon fiber-reinforced PAEK composites: a review. *Mater Today Commun*. 2022;32:104036. doi:10.1016/j.mtcomm.2022.104036

5. Bonmatin M, Chabert F, Bernhart G, Cutard T, Djilali T. Ultrasonic welding of CF/PEEK composites: influence of welding parameters on interfacial temperature profiles and mechanical properties. *Compos A: Appl Sci Manuf*. 2022;162:107074. doi:10.1016/j.compositesa.2022.107074

6. Arquier R, Sabatier H, Iliopoulos I, Régnier G, Miquelard-Garnier G. Role of the inter-ply microstructure in the consolidation quality of high-performance thermoplastic composites. *Polym Compos*. 2024;45:1218-1227. doi:10.1002/pc.27847

7. Baumard T, Lévy A, El Rassy E, et al. Development of a coupled diffusion-crystallization-degradation model during welding of paek thermoplastics. *23rd International Conference on Composite Materials (ICCM23)*; ICCM 23. 2023.

8. Yassin K, Hojjati M. Processing of thermoplastic matrix composites through automated fiber placement and tape laying methods: a review. *J Thermoplast Compos Mater*. 2018;31:1676-1725. doi:10.1177/0892705717738305

9. Pérez-Martín H, Mackenzie P, Baidak A, Ó Brádaigh CM, Ray D. Crystallisation behaviour and morphological studies of PEKK and carbon fibre/PEKK composites. *Compos A: Appl Sci Manuf*. 2022;159:106992. doi:10.1016/j.compositesa.2022.106992

10. Martin I, Saenz del Castillo D, Fernandez A, Güemes A. Advanced thermoplastic composite manufacturing by in-situ consolidation: a review. *J Compos Sci*. 2020;4:149. doi:10.3390/jcs4040149

11. Courvoisier E, Bicaba Y, Colin X, Water absorption in PEEK and PEI matrices. Contribution to the understanding of water-polar group interactions. *AIP Conf Proc*. 2016;1736:020036. doi:10.1063/1.4949611

12. Grayson MA, Pao PS, Wolf CJ. Transport of methylene chloride in poly(aryl-ether-ether-ketone) (PEEK). *J Polym Sci B*. 1987;25:935-945. doi:10.1002/polb.1987.090250416

13. Grayson MA, Wolf CJ. The solubility and diffusion of water in poly(aryl-ether-ether-ketone) (PEEK). *J Polym Sci B*. 1987;25:31-41. doi:10.1002/polb.1987.090250103

14. Wang Q, Springer GS. Moisture absorption and fracture toughness of PEEK polymer and graphite fiber reinforced PEEK. *J Compos Mater*. 1989;23:434-447. doi:10.1177/002199838902300501

15. Batista NL, Rezende MC, Botelho EC. The influence of crystallinity on the weather resistance of CF/PEEK composites. *Appl Compos Mater*. 2021;28:235-246. doi:10.1007/s10443-020-09863-x

16. Jung H, Bae KJ, Jin J, et al. The effect of aqueous polyimide sizing agent on PEEK based carbon fiber composites using experimental techniques and molecular dynamics simulations. *Funct Compos Struct*. 2020;2:025001. doi:10.1088/2631-6331/ab8884

17. Yildirim C, Tabrizi IE, Al-Nadhari A, Topal S, Beylergil B, Yildiz M. Characterizing damage evolution of CF/PEKK composites under tensile loading through multi-instrument structural

health monitoring techniques. *Compos A: Appl Sci Manuf.* 2023; 175:107817. doi:10.1016/j.compositesa.2023.107817

18. Gardner KH, Hsiao BS, Matheson RR, Wood BA. Structure, crystallization and morphology of poly (aryl ether ketone ketone). *Polymer.* 1992;33:2483-2495. doi:10.1016/0032-3861(92)91128-O

19. Ark Dent Kepstan® PEKK Polymer Range. Arkema. 2022 https://www.extremematerials-arkema.com/en/product-families/kepstan-pekk-polymer-range/ (accessed March 8, 2022)

20. Paul S, Legner W, Krenkow A, et al. Chemical contamination sensor for phosphate Ester hydraulic fluids. *Int J Aerosp Eng.* 2010;2010:e156281. doi:10.1155/2010/156281

21. Eastman. Safety Data Sheet - Skydrol® LD4 Fire Resistant Hydraulic Fluid. 2019.

22. Sugita Y, Winkelmann C, La Saponara V. Environmental and chemical degradation of carbon/epoxy lap joints for aerospace applications, and effects on their mechanical performance. *Compos Sci Technol.* 2010;70:829-839. doi:10.1016/j.compscitech.2010.01.021

23. Tracy J, Yin Y, Yang J, Osborne JC, Blohowiak KY, Dauskardt R. Environmentally assisted crack growth in adhesively bonded composite joints. *Compos A: Appl Sci Manuf.* 2017;102:368-377. doi:10.1016/j.compositesa.2017.08.018

24. Markatos DN, Tserpes KI, Rau E, Markus S, Ehrhart B, Sp P. The effects of manufacturing-induced and in-service related bonding quality reduction on the mode-I fracture toughness of composite bonded joints for aeronautical use. *Composites, Part B.* 2013;45:556-564. doi:10.1016/j.compositesb.2012.05.052

25. Buggy M, O'Byrne K. Effects of skydrol (a hydraulic fluid) on the network structure of TGDDM/DDS-based resins. *J Appl Polym Sci.* 1997;65:2025-2030. doi:10.1002/(SICI)1097-4628(19970906)65:10<3.0.CO;2-3

26. La Saponara V. Environmental and chemical degradation of carbon/epoxy and structural adhesive for aerospace applications: Fickian and anomalous diffusion. *Arrhenius Kinetics Compos Struct.* 2011;93:2180-2195. doi:10.1016/j.compstruct.2011.03.005

27. Stober EJ, Seferis JC, Keenan JD. Characterization and exposure of polyetheretherketone (PEEK) to fluid environments. *Polymer.* 1984;25:1845-1852. doi:10.1016/0032-3861(84)90260-X

28. Dominguez S. *Relation structure/propriétés de polymères et mélanges thermoplastiques thermostables - Applications Aéronautiques Hautes Températures.* These de doctorat; 2013.

29. Horn WJ, Shaikh FM, Soeganto A. Degradation of mechanical properties of advanced composites exposed to aircraft environment. *AIAA Journal.* 1989;27:1399-1405. doi:10.2514/3.10277

30. Ma C-CM, Lee C-L, Tai N-H. Chemical resistance of carbon fiber-reinforced poly(ether ether ketone) and poly(phenylene sulfide) composites. *Polym Compos.* 1992;13:435-440. doi:10.1002/pc.750130606

31. Pritchard G, Randles SJ. The interaction of liquids with polyaryl ether ether ketone composites. *Plast Rubber Compos.* 1995; 24:175-180.

32. Tencé-Girault S, Quibel J, Cherri A, et al. Quantitative structural study of cold-crystallized PEKK. *ACS Appl Polym Mater.* 2021;3:1795-1808. doi:10.1021/acsapm.0c01380

33. Lesimple G, Iliopoulos I, Marijon J-B, Fayolle B. Full characterization of water transport properties in Polyetherketoneketone (PEKK). *ACS Appl Polym Mater.* 2023;5:302-310. doi:10.1021/acsapm.2c01515

34. Chamis CC, Sinclair JH. 10 off-Axis tensile test for intralaminar shear characterization of fiber composites. 1976.

35. NF EN 2489. Série aérospatiale—Plastiques renforcés de fibres - Détermination de l'action des fluides d'essais. 1996.

36. Jones E, Iadicola M. *A good practices guide for digital image correlation.* 1st ed. International Digital Image Correlation Society; 2018. doi:10.32720/idics/gpg.ed1/print.format

37. Merzkirch M, Foecke T. 10° off-Axis tensile testing of carbon fiber reinforced polymers using digital image correlation. *Mechanics of Composite and Multi-Functional Materials.* Vol 5. Springer; 2020:55-62. doi:10.1007/978-3-030-30028-9_8

38. Lesimple G. *Interaction du PEKK et des composites PEKK/FC avec l'eau et le Skydrol.* HESAM Université; 2023.

39. Weitsman YJ, Guo Y-J. A correlation between fluid-induced damage and anomalous fluid sorption in polymeric composites. *Compos Sci Technol.* 2002;62:889-908. doi:10.1016/S0266-3538(02)00032-5

40. Gagani AI, Echtermeyer AT. Fluid diffusion in cracked composite laminates – analytical, numerical and experimental study. *Compos Sci Technol.* 2018;160:86-96. doi:10.1016/j.compscitech.2018.03.025

41. Cantwell WJ, Davies P, Kausch HH. The effect of cooling rate on deformation and fracture in IM6/PEEK composites. *Compos Struct.* 1990;14:151-171. doi:10.1016/0263-8223(90)90028-D

42. Tsukada T, Minakuchi S, Takeda N. Identification of process-induced residual stress/strain distribution in thick thermoplastic composites based on in situ strain monitoring using optical fiber sensors. *J Compos Mater.* 2019;53:3445-3458. doi:10.1177/0021998319837199

43. Pradere C, Sauder C. Transverse and longitudinal coefficient of thermal expansion of carbon fibers at high temperatures (300–2500K). *Carbon.* 2008;46:1874-1884. doi:10.1016/j.carbon.2008.07.035

44. Parlevliet PP, Bersee HEN, Beukers A. Residual stresses in thermoplastic composites—a study of the literature—part I: formation of residual stresses. *Compos A: Appl Sci Manuf.* 2006;37:1847-1857. doi:10.1016/j.compositesa.2005.12.025

45. Parlevliet PP, Bersee HEN, Beukers A. Residual stresses in thermoplastic composites – a study of the literature. Part III: effects of thermal residual stresses. *Compos A: Appl Sci Manuf.* 2007;38:1581-1596. doi:10.1016/j.compositesa.2006.12.005

46. Kim J-K, Mai Y-W, Mai Y-W. Chapter 7 - improvement of transverse fracture toughness with interface control. In: Kim J-K, Mai Y-W, Mai Y-W, eds. *Engineered Interfaces in Fiber Reinforced Composites.* Elsevier Science Ltd; 1998:279-327. doi:10.1016/B978-008042695-2/50008-7

47. Merzkirch M, Foecke T. 10° off-axis testing of CFRP using DIC: a study on strength, strain and modulus. *Composites, Part B.* 2020;196:108062. doi:10.1016/j.compositesb.2020.108062

SUPPORTING INFORMATION

Additional supporting information can be found online in the Supporting Information section at the end of this article.